Electrodeposition of Zinc from Binary $ZnCl_2$-$DMSO_2$ Molten Electrolyte at Room Temperature

Chao-Chen Yang[a] and Min-Fong Shu[b]

[a] Department of Chemical Engineering, National Yunlin University of Science and Technology, Touliu, Yunlin, Taiwan, R.O.C.
[b] Graduate School of Engineering Science and Technology (Doctoral Program), National Yunlin University of Science and Technology, Touliu, Yunlin, Taiwan, R.O.C.

Reprint requests to C.-C. Y.; Fax: 886-5-531-2071; E-mail: prof.ccyang@gmail.com

Z. Naturforsch. **62a,** 754 – 760 (2007); received April 27, 2007

The electrochemical behaviour of zinc on copper, platinum, and tungsten working electrodes was investigated in a binary $ZnCl_2$-$DMSO_2$ room temperature molten salt electrolyte in the temperature range of 60 – 80 °C. Various over-potentials, −0.1, −0.2, −0.3, −0.4, and −0.5 V, were chosen as deposition potentials. The nucleation/growth of zinc changed from progressive to instantaneous if the over-potentials increased from low to high level. The surface morphology and crystal structure of the deposited layer were investigated using scanning electron microscopy (SEM) and X-ray diffraction (XRD). Moreover, larger grain size and hexagonal close packing of the zinc layer at −0.5 V were observed by transmission electron microscopy (TEM) with electron diffraction mapping.

Key words: Room Temperature Molten Salt; $ZnCl_2$-$DMSO_2$ Electrolyte; Progressive Nucleation; Instantaneous Nucleation.

1. Introduction

Zinc can be obtained by electrodeposition from aqueous or non-aqueous electrolytes. Generally, when an aqueous electrolyte is applied lower current efficiency is observed, which is caused by hydrogen production in the over-potential. On the other hand non-aqueous electrolyte, including molten chlorozincate, gives high zinc purity forms complex solvates with better solubility. Moreover, it possesses other physical advantages such as high electrical conductivity, a wide electrochemical window, low density, and low vapour pressure.

Room temperature molten salts, including inorganic and organic mixtures, have been reported in several papers [1 – 5]. E. g., electrodepositing zinc or zinc alloys in the room temperature molten salt $ZnCl_2$-EMIC (1-ethyl-3-methylimidazolium chloride) been studied by Sun et al. The molten salt systems $CoCl_2$-$ZnCl_2$-BPC (butylpyridinium chloride) and $CoCl_2$-$AlCl_3$-BPC have also been used for metal electrodeposition [6, 7]. However, the preparation and conservation of organic chloride salts are not easy. Also it is expensive to synthesize them. Molten $AlCl_3$-$DMSO_2$ (dimethylsufone) with added $TiCl_3$ as electrolyte was used for anodic dissolution by Legrand et al. [8, 9]. These authors indicated that $DMSO_2$ could serve as a good solvent in inorganic mixtures. A previous report [10] indicates that the $ZnCl_2$-$DMSO_2$ binary system has a good conductivity and density.

In this study a room temperature molten chlorozincate ($ZnCl_2$-$DMSO_2$) was used as electrolyte to electrodeposit zinc. The morphological structure and the nucleation/growth mechanism of the deposited layer has been investigated.

2. Experimental

$ZnCl_2$ (Merck, anhydrous, 98%) and $DMSO_2$ (Acros, 98%) were stored in a glove compartment filled with desiccated nitrogen gas. The preparation of the $ZnCl_2$-$DMSO_2$ melt and the pretreatment of the chemicals have been detailed in [10]. The composition of the molten salt electrolyte mixing at various operating temperatures depends on the phase diagram of binary system [10]. A potentiostat-galvanostat (EG & G, Princeton Applied Research model 273A) was used for the electrochemical measurement and electrodeposition of the Zn layer on a Cu substrate. Copper (geometric area = 0.63617 mm^2, Nilaco Co., 99.99%), platinum (geometric area = 1.767 mm^2, Nilaco Co., 99.99%), and tungsten (geometric area = 0.7853 mm^2, Nilaco Co., 99.95%) were used as the working electrodes. These were also taken to investigate the electrochemical reaction behaviour. The Zn/$[ZnCl_4]^{2-}$ electrode containing the 50 : 50 mol% $ZnCl_2$-$DMSO_2$ melt with inserting zinc wire (0.8 mm diameter, Nilaco Co., 99.99%) in a glass tube was prepared as reference and counter electrode.

The chronoampermetry technique was used to measure current-time curves at various over-potentials. In order to study the nucleation/growth mechanism of metallic zinc, the theoretical curves of instantaneous/progressive nucleation

$$(i/i_M)^2 = 1.9542\{1-\exp[-1.2564(t/t_M)]\}^2/(t/t_M) \quad \text{(instantaneous)}, \qquad (1)$$

$$(i/i_M)^2 = 1.2254\{1-\exp[-2.3367(t/t_M)^2]\}^2/(t/t_M) \quad \text{(progressive)}, \qquad (2)$$

were plotted and compared with the experimentally measured curves. The morphology of the electrodeposited layers was measured by scanning electron microscopy (SEM), and the Zn layer crystalline structure was identified by X-ray diffraction (XRD). Transmission electron microscopy (TEM) was usede for investigating the zinc metallic crystalline structure and orientation.

3. Results and Discussion

The cyclic voltammograms of zinc, which is electrodeposited on platinum, tungsten, and copper electrodes at 70 °C with a scanning rate of 25 mV/s, are shown in Figure 1. The results reveal that the O1 peak and the R1 zone have pronounced zinc oxidation and reduction reactions in the 50 : 50 mol% $ZnCl_2$-$DMSO_2$ molten salt. The three electrodes show similar results for the electrochemical behaviour. The reaction rates of the working electrodes are in decreasing order: copper larger than tungsten larger than platinum. In addition, peaaks in the oxidation and reduction reactions of copper at O2 and R2 were obtained as shown in Figure 1. These voltammograms reveal that the reduction of zinc can be achieved at a deposition potential ranging from −0.5 to −0.1 V. In the molten salt system $ZnCl_2$-$DMSO_2$ the reaction solvated ions and the zinc reduction can be represented by the following equations:

$$2ZnCl_2 + n(CH_3)_2SO_2 = [ZnCl_4]^{2-} + Zn[(CH_3)_2SO_2]_n^{2+}, \qquad (3)$$

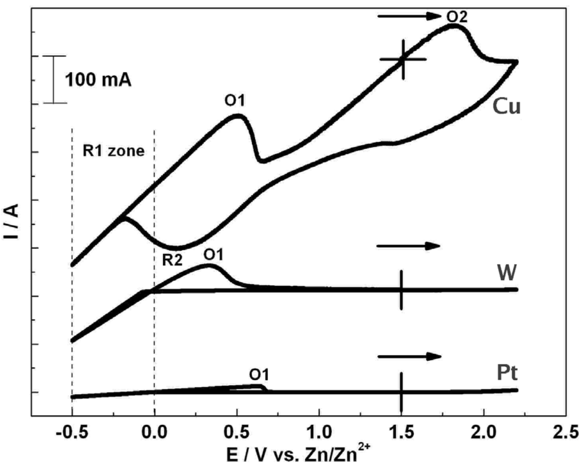

Fig. 1. Cyclic voltammograms recorded at the working electrodes Pt, W, and Cu in 50 : 50 mol% $ZnCl_2$-$DMSO_2$ molten salt at 70 °C with 25 mV/s scan rate.

$$Zn[(CH_3)_2SO_2]_n^{2+} + 2e^- = Zn + n(CH_3)_2SO_2. \qquad (4)$$

From these equations it is understandable that the main ions in the $ZnCl_2$-$DMSO_2$ system are the $[ZnCl_4]^{2-}$ and $Zn[(CH_3)_2SO_2]_n^{2+}$ complexes. As the $[ZnCl_4]^{2-}$ complex ion has a higher stability, the $Zn[(CH_3)_2SO_2]_n^{2+}$ complex ion plays the dominant role in the electrochemical reaction. The deposition reaction of Zn is shown in (4). Similar reactions were obtained in the $AlCl_3$-$DMSO_2$ system [8, 9]. It is therefore apparant that $DMSO_2$ can be used as a non-ionic solvent for metal chloride.

Cyclic voltammograms of platinum and tungsten electrodes at different temperatures (60 – 80 °C) in the 50 : 50 mol% $ZnCl_2$-$DMSO_2$ molten salt are shown in Figs. 2A and 2B, respectively. The largest values for the current could be obtained by using these electrodes. Apparantly the oxidation-reduction rates of ionic species are determined by the activation energy of zinc metal involving thermal effect as driving force. 44.47 kJ/mol at E_{Pt} and the 52.62 kJ/mol at E_W are measured and interpreted with Arrhenius-type equations which are shown in the inserted plots of Figs. 2A and 2B. The results indicate that the activation energy of the ionic reaction on the Pt electrode is lower than that on the W electrode. Due to the lower activation energy the rate constant from the state of an activated complex is higher. Furthermore, the ionic interaction is related to the stability of the complex and to the charge transfer at the electrode. This also indicates an activation energy for the inter-ionic reaction.

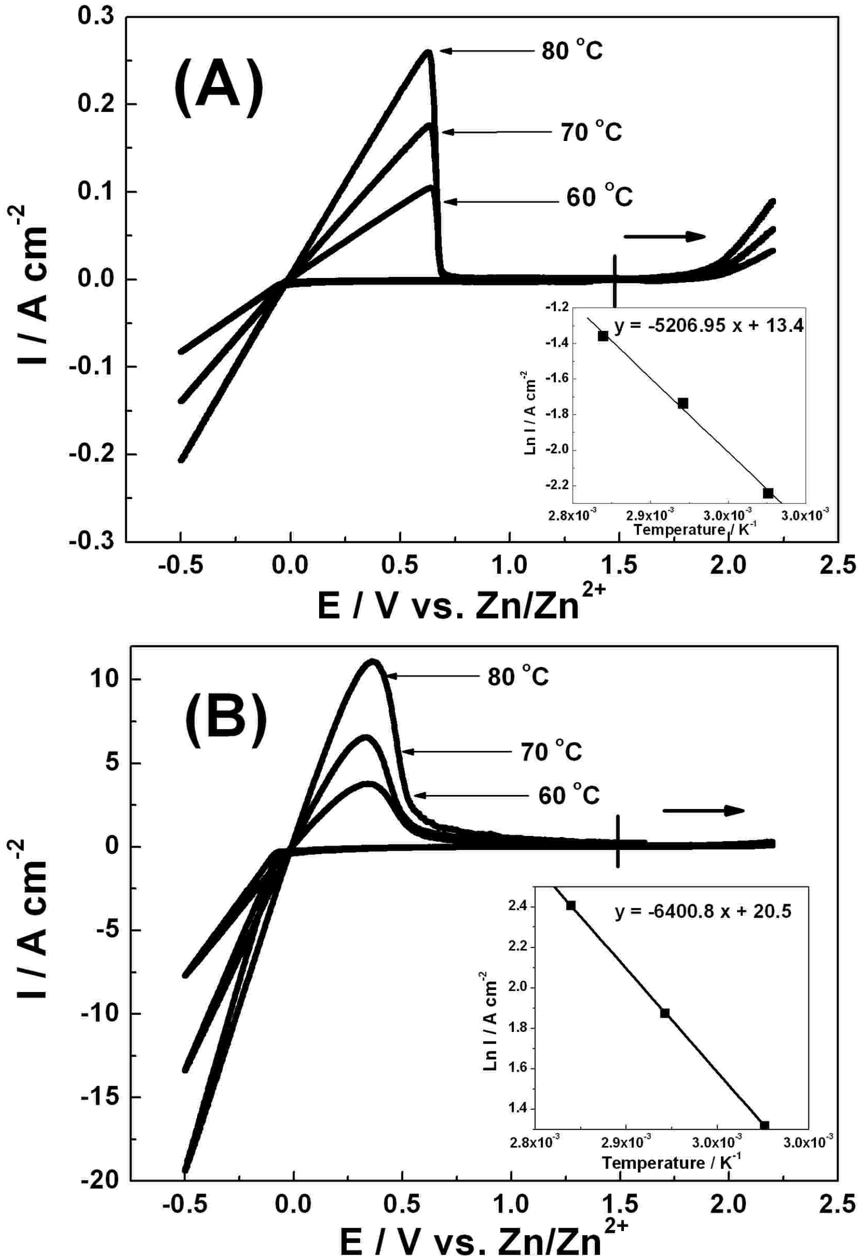

Fig. 2. Cyclic voltammograms recorded at the working electrodes (A) platinum and (B) tungsten in 50 : 50 mol% $ZnCl_2$-$DMSO_2$ melt at various temperatures with 25 mV/s scan rate.

The electrochemical nucleation concept can be explained by observing the behaviour of the charge current at the electrode-solution interface. This process has three parts. The first step is the accumulation of the positive charges, resulting in a sharp increase of the current on the electrode surface. Second, the current is decreased by the formation of negative charges because of the potential across the interface and solution. The third step is the formation of a nucleation increase as positive ions or positive ion complexes move to the surface of the electrode due to the existence of negative charges at the surface. This also causes the current to slowly decrease at the electrode surface. The electrochemical nucleation is mainly controlled by this third step.

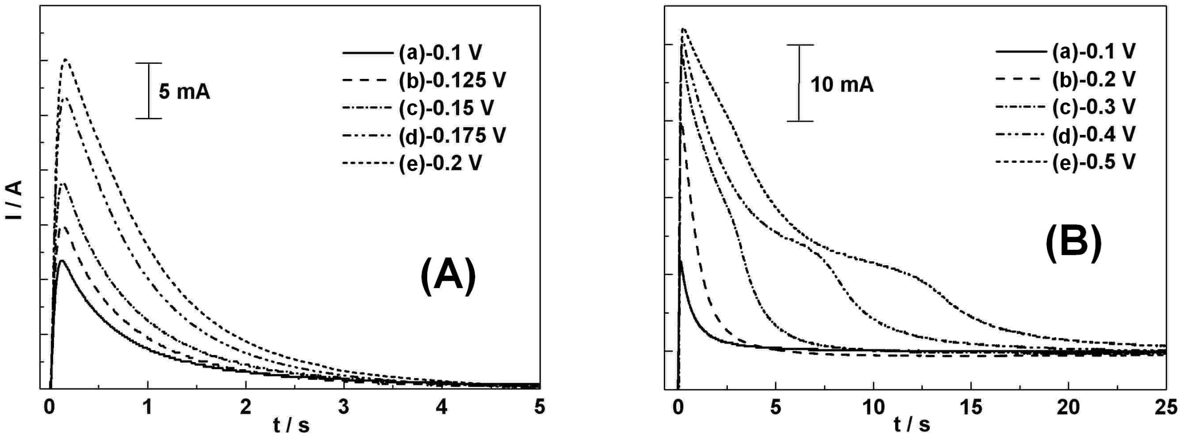

Fig. 3. Current-time transients resulting from chronoamperometry experiments recorded on the copper electrode in a binary 50 : 50 mol% $ZnCl_2$-$DMSO_2$ melt at 70 °C. (A) Applied potentials are from −0.1 to −0.2 V; (B) applied potentials are from −0.1 to −0.5 V.

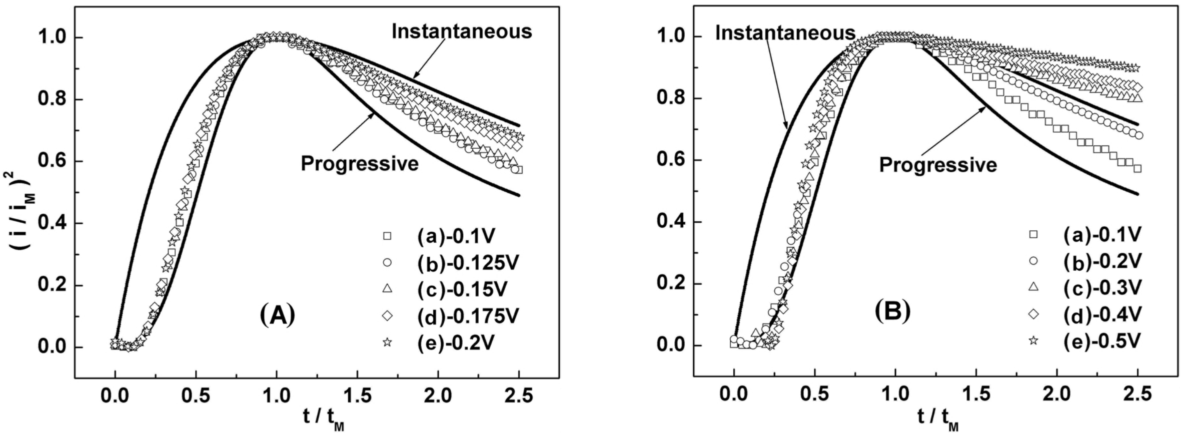

Fig. 4. Comparison of the dimensionless experimental current-time transients derived from Fig. 3 with the theoretical models for the 3-D nucleation process. Solid lines are from the theoretical model of equations (1) and (2). (A) Applied potentials are from −0.1 to −0.2 V; (B) applied potentials are from −0.1 to −0.5 V.

Figures 3A and 3B show current-time plots of deposited zinc on a copper electrode at 70 °C while applying a constant potential whose values range from −0.5 to −0.1 V. These plots were done by using a chronoamperometry program. The results reveal that the nucleation mechanism varies according to the applied potential. In all cases, the current abruptly increased from the range of the initial current to the maximum current (i_M), and we could obtain the maximum time (t_M) from observing i_M. Moreover, the current decreased with increasing time after i_M. The current-time curve represents the nucleation and growth of zinc metal on a copper electrode. It is also seen that the value of i_M in the current-time curve increase with increasing over-potential. A report [11] on the investigation of the electrodeposition of zinc in an aqueous electrolyte also showed similar results for the current time curve. In addition, we observe that the current change with respect to the nucleation/growth rate slowly reaches a steady-state at higher over-potential. According to the Cottrell behaviour, the current decays slowly with time while meantime the diffusion layer becomes thicker. Moreover, we have used the three-dimensional instantaneous and progressive nucleation theories, such as shown in (1) and (2) and have simulated a reference curve. These results are shown as black lines in Figs. 4A and 4B. In addition, the chronoamperometry curve from Figs. 3A

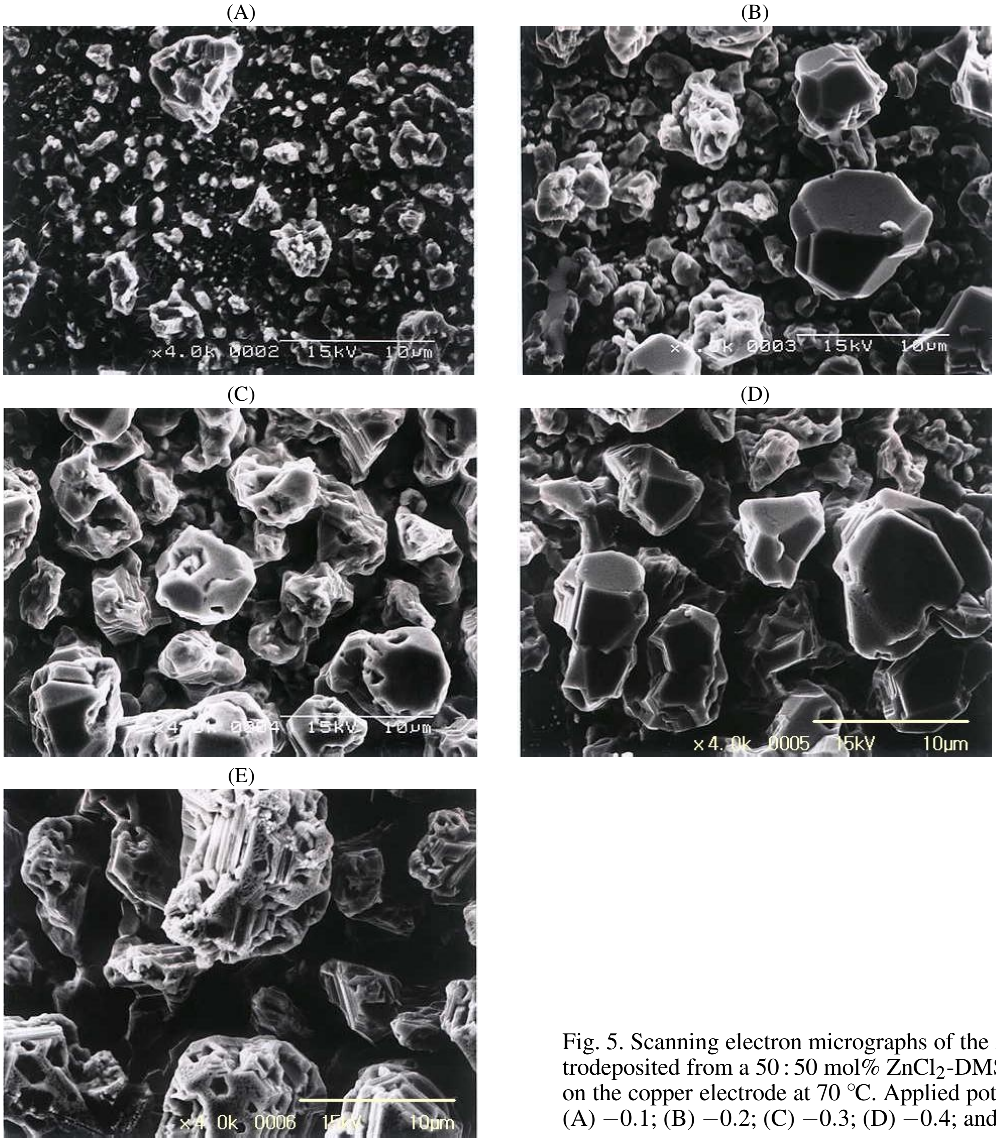

Fig. 5. Scanning electron micrographs of the zinc layer electrodeposited from a 50 : 50 mol% $ZnCl_2$-$DMSO_2$ electrolyte on the copper electrode at 70 °C. Applied potentials (V) are: (A) −0.1; (B) −0.2; (C) −0.3; (D) −0.4; and (E) −0.5.

and 3B was transferred to three-dimensional instantaneous and progressive nucleation curves as shown in the points of Figs. 4A and 4B. The results indicate that the instantaneous nucleation/growth mechanism also holds at a higher over-potential. Hence, a higher amount of complex ions has diffused through the electrode double layer. A thicker diffusion layer is also obtained at higher over-potential. The above results of electrochemical nucleation and growth are similar to those obtained in the study of electrodeposition of Zn-Co-Dy alloys from the 50 : 50 $ZnCl_2$-EMIC-1.687 mol% $CoCl_2$-1.114 mol% $DyCl_3$ molten electrolyte at higher over-potential [12]. In the literature is has been shown that the progressive nucleation changes to instantaneous nucleation as observed on nickel and copper electrodes at −1.3 V to −0.8 V.

The zinc nucleation and growth have been observed on copper electrodes, such as demonstrated with the above results. Applied deposition potentials would affect the surface morphology and the crystal orientation of the zinc deposit. The surface morphology of the electrodeposited layers at various applied potentials −0.1, −0.2, −0.3, −0.4, and −0.5 V, are shown in Figs. 5A – E. The results reveal that a larger grain

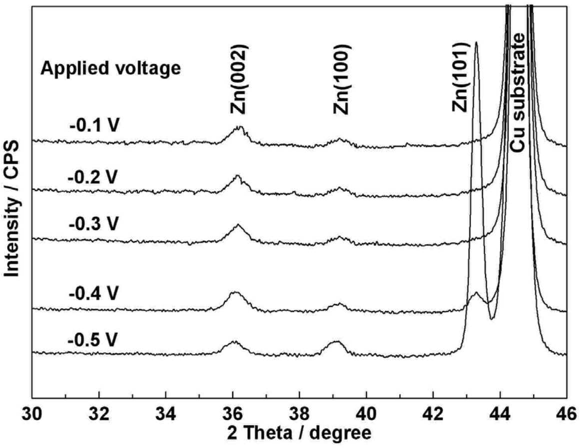

Fig. 6. X-Ray diffraction patterns of the zinc layer electrodeposited from a 50 : 50 mol% $ZnCl_2$-$DMSO_2$ electrolyte on the copper electrode at 70 °C. Applied potentials (V) are: (A) −0.1; (B) −0.2; (C) −0.3; (D) −0.4; and (E) −0.5.

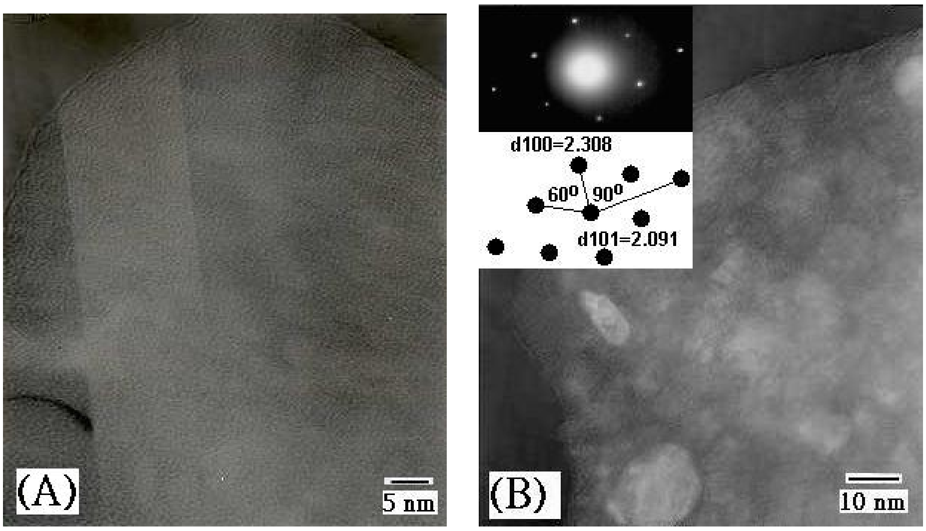

Fig. 7. Transmission electron micrographs of the zinc layer electrodeposited from the 50 : 50 mol% $ZnCl_2$-$DMSO_2$ electrolyte on the copper electrode at 70 °C. (A) The applied voltage is −0.1 V. (B) The applied voltage is −0.5 V. The inserted image is the diffraction pattern.

size is observed at higher over-potential from −0.5 V to −0.3 V. This is due to the instantaneous nucleation/growth as shown in Figure 4B. Moreover, a smaller grain size of the deposited layer at −0.1 V and −0.2 V is shown in Figs. 5A and 5B. We have compared the surface morphology of electrodeposited layers with the nucleation/growth behaviour of three-dimensional processes. It is observed that the surface structure and the mechanism of nucleation/growth of deposited layers depend on the applied potential. Also this reveals that the electroplated parameters of the molten salt electrolyte can be applied to an industrial production of metal. On the other hand, we used XRD analysis to observe the crystal structure of the deposited layers on the copper electrode at various applied over-potentials, as shown in Figure 6. It is clear that the (002) and (100) crystalline peaks can be observed for applied over-potentials from −0.5 to −0.1 V. Furthermore, a sharp crystalline (101) peak at −0.4 V or −0.5 V is observed. The electrodeposited zinc metal with these crystalline peaks has a hexagonal close packed (hcp) unit cell.

Transmission electron microscopy (TEM) images and electron diffraction patterns of zinc deposited layers at −0.1 V and −0.5 V are shown in Figs. 7A and 7B, respectively. They show that a uniform order of crystal structure on grain boundaries was obtained (Fig. 7A). Moreover, a larger grain size of the crystal could be observed if an over-potential of −0.5 V was applied (Fig. 7B). These were identified as having hcp structures, as shown in the inset of Figure 7B. Similar results were obtained with SEM. Moreover, a tiny crystal structure was observed if the applied potential was −0.1 V, whereas at −0.5 V, a larger grain size and hcp structure of the deposited layer were seen.

4. Conclusion

A binary $ZnCl_2$-$DMSO_2$ molten salt electrolyte was shown to be capable of electrodepositing zinc with satisfactory results. The properties including the electrochemical behaviour of the electrolyte and the nucleation/growth mechanism of the zinc deposited layers were identified through cyclic voltammetry and chronoampermetry. The results showed that solvents such as $DMSO_2$ mixed with $ZnCl_2$ forming a complex ion in the chlorozincate salt could react on the electrode surface. The instantaneous nucleation/growth and larger grain size of the electrodeposited zinc were observed at higher over-potential by using a 50 : 50 mol% $ZnCl_2$-$DMSO_2$ electrolyte. Moreover, the (002), (100), and (101) crystal planes of the zinc deposited layers were observed by XRD analysis. Meanwhile, a hcp structure of the layer at −0.5 V was identified by the use of electron diffraction and TEM images.

Acknowledgement

The authors acknowledge financial support from the National Science Council under contract number NSC-90-2214-E-224-008.

[1] Y. F. Lin and I. W. Sun, Electrochim. Acta **44**, 2771 (1999).
[2] M. C. Lin, P. Y. Chen, and I. W. Sun, J. Electrochem. Soc. **148**, C653 (2001).
[3] J. F. Huang and I. W. Sun, J. Electrochem. Soc. **150**, E299 (2003).
[4] M. H. Yang, M. C. Yang, and I. W. Sun, J. Electrochem. Soc. **150**, C544 (2003).
[5] J. F. Huang and I. W. Sun, J. Electrochem. Soc. **151**, C8 (2004).
[6] N. Koura, T. Endo, and Y. Idemoto, J. Non-Cryst. Solid **205** – **207**, 650 (1996).
[7] C. C. Yang, T. H. Wu, and M. F. Shu, Z. Naturforsch. **59b**, 519 (2004).
[8] L. Legrand, E. Chassaing, A. Chausse, and R. Messina, Electrochim. Acta **43**, 3109 (1998).
[9] L. Legrand, A. Chausse, and R. Messina, Electrochim. Acta **46**, 2407 (2001).
[10] M. F. Shu, H. Y. Hsu, and C. C. Yang, Z. Naturforsch. **58a**, 451 (2003).
[11] J. Yu, L. Wang, L. Su, X. Ai, and H. Yang, J. Electrochem. Soc. **150**, C19 (2003).
[12] H. Y. Hsu and C. C. Yang, Z. Naturforsch. **58b**, 139 (2002).